Inorg. Chem. **2007**, *46*, 8088–8097

Inorganic Chemistry
Article

New Fluorescent Chemosensors for Heavy Metal Ions Based on Functionalized Pendant Arm Derivatives of 7-Anthracenylmethyl-1,4,10-trioxa-7,13-diazacyclopentadecane

M. Carla Aragoni,[†] Massimiliano Arca,[†] Andrea Bencini,[‡] Alexander J. Blake,[§] Claudia Caltagirone,[†] Andrea Danesi,[‡] Francesco A. Devillanova,[†] Alessandra Garau,[†] Thomas Gelbrich,[||] Francesco Isaia,[†] Vito Lippolis,[*,†] Michael B. Hursthouse,[||] Barbara Valtancoli,[‡] and Claire Wilson[§]

Dipartimento di Chimica Inorganica ed Analitica, Università degli Studi di Cagliari,
S.S. 554 Bivio per Sestu, 09042 Monserrato (CA), Italy, Dipartimento di Chimica, Università di
Firenze, Polo Scientifico, Via della Lastruccia 3, 50019 Sesto Fiorentino, Florence, Italy,
School of Chemistry, The University of Nottingham, University Park, Nottingham NG7 2RD, U.K.,
and Department of Chemistry, The University of Southampton, Highfield,
Southampton SO17 1BJ, U.K.

Received April 5, 2007

Two new ligands 7-anthracenylmethyl-13-methylpyridyl-1,4,10-trioxa-7,13-diazacyclopentadecane (**L**^{4}) and 7-anthracenylmethyl-13-(2,2-dimethyl-2-hydroxyethyl)-1,4,10-trioxa-7,13-diazacyclopentadecane (**L**^{5}) have been synthesized and characterized. Both derive from 7-anthracenylmethyl-1,4,10-trioxa-7,13-diazacyclopentadecane (**L**^{3}) and differ for having a differently functionalized pendant arm covalently attached to the remaining secondary nitrogen donor of the macrocyclic framework. The protonation and coordination behavior of **L**^{4}, **L**^{5}, and the unbranched **L**^{3} with metal ions have been studied in MeCN/H_2O (1:1 v/v, 298.1 K, $I = 0.1$ M) using potentiometric methods. The crystal structures of **L**^{3}, $[(H_2\mathbf{L}^3)(H\mathbf{L}^3)](ClO_4)_3$, and the complex $[Cd\mathbf{L}^3(NO_3)_2]$ have been determined by single-crystal X-ray methods. The fluorescent behavior of **L**^{3}–**L**^{5} in the presence of Cu^{II}, Zn^{II}, Cd^{II}, Hg^{II}, and Pb^{II} has been studied as a function of pH in MeCN/H_2O (1:1 v/v). The presence of Cu^{II}, Hg^{II}, or Pb^{II} does not affect the fluorescent behavior observed for the three free ligands upon changing the pH. Interestingly, the fluorescent emission of **L**^{3} and **L**^{5} is selectively enhanced only in the presence of Cd^{II} at basic pH. The same effect is observed for **L**^{4} in the presence of Cd^{II} or Zn^{II} at about pH 7.

Introduction

The development of artificial chemosensors − discrete molecules that selectively recognize and signal to an external operator the presence of a specific analyte in a complex matrix − is one of the main technological applications of supramolecular chemistry, and it is continuing strongly and gaining in momentum. The intense interest in this field is driven by the growing demand for extremely sensitive and selective analytical tools for the detection and monitoring of charged and neutral substrates in biological, environmental, and industrial waste effluent samples.

Excellent results have been achieved with fluorescent chemosensors, which offer many advantages with respect to other types of chemosensors in terms of selectivity, sensitivity, response time, and cost.[1−10] A common fluores-

---

[*] To whom correspondence should be addressed. E-mail: lippolis@unica.it. Phone: +39 070 6754467. Fax: +39 070 6754456.

[†] Università degli Studi di Cagliari.

[‡] Università di Firenze.

[§] The University of Nottingham.

[||] The University of Southampton.

(1) *Chemosensors of Ions and Molecular Recognition*, Czarnik, A. W., Desvergene, J.-P. Eds.; NATO ASI Ser., Ser. C; Kluwer Academic Publishers: Dordrecht, The Netherlands, 1997; Vol. 492.

(2) de Silva, A. P.; Gunaratne, H. Q. G.; Gunnlaugsson, T.; Huxley, A. J. M.; McCoy, C. P.; Rademacher, J. T.; Rice, T. E. *Chem. Rev.* **1997**, *97*, 1515.

(3) (a) Fabbrizzi, L.; Licchelli, M.; Taglietti, A. *Dalton Trans.* **2003**, 3471−3479. (b) Amendola, V.; Fabbrizzi, L.; Foti, F.; Licchelli, M.; Mangano, C.; Pallavicini, P.; Poggi, A.; Sacchi, D.; Taglietti, A. *Coord. Chem. Rev.* **2006**, *250*, 273.

(4) Kimura, E.; Koike, T. *Chem. Soc. Rev.* **1998**, *27*, 179.

(5) Prodi, L. *New. J. Chem.* **2005**, *29*, 20.

(6) Prodi, L.; Bolletta, F.; Montalti, M.; Zaccheroni, N. *Coord. Chem. Rev.* **2000**, *205*, 59.

(7) Rurack, K. *Spectrochim. Acta, Part A* **2001**, *57*, 2161.

(8) *J. Mater. Chem.* **2005**, *15*, 2617−2976. Theme Issue: Fluorescent Sensors.

10.1021/ic700657j CCC: $37.00

cent *conjugated* chemosensor is generally constituted by a fluorogenic fragment (signaling unit) that is covalently linked, through an appropriate spacer, to a guest-binding site (receptor unit).[1−11]

The recognition of the target species by the receptor unit as a result of a selective host−guest interaction between the two is converted into an enhancement or quenching of the fluorophore emission.

The choice of the read-out or signaling unit can be critical to both the performance and the selectivity/specificity of the sensor, especially if a direct interaction between the fluorophore and the target species is implied. However, the sensor selectivity/specificity would be determined solely or mainly by the nature of the receptor unit, whereas the transduction mechanism that is triggered upon the host−guest interaction and the sensitivity or sensor performance would be determined exclusively by the fluorogenic fragment, when the latter does not interact with the target species.

This is the case for many metal cation sensors that feature anthracenyl derivatives of aza−oxa macrocyclic ligands in which the fluorescence emission is determined by a photoinduced electron transfer (PET) between the anthracene fragment and the tertiary nitrogen atom of the macrocyclic moiety. The main strategy in the design of specific and selective fluorescent chemosensors of this type commonly involves modeling the structure of the receptor units so as to better match the binding properties of the target metal cation.

1,4,10-trioxa-7,13-diazacyclopentadecane (**L^1**) is commercially available, and because of its marked tendency to bind different metal ions (alkali and alkaline earths, transition metals and lanthanides)[12−18] it has already been used as a receptor unit in redox and fluorescent *conjugated* chemosensors.[19−26] Normally, fluorescent conjugated chemosensors based on polyaza or aza−oxa macrocyclic receptors such as **L^1** feature, for obvious synthetic reasons, all of the nitrogen donor atoms belonging to the macrocyclic framework functionalized with the same type of signaling fluorogenic unit (**L^2** in Figure 1 reported by Martínez-Máñez and co-workers, which features two anthracenylmethyl units attached to the secondary nitrogen atoms of **L^1**; the emission intensity of **L^2** is selectively enhanced in the presence of Hg^{II} at basic pH in 1,4-dioxane/H_2O, 70:30 v/v).[22−26] Martínez-Máñez and co-workers have also reported difunctionalized polyaza or aza−oxa macrocyclic receptors that contain more than one type of signaling unit; these systems can be considered as multiple-sensing chemosensors capable of displaying two or more macroscopic observable events upon the addition of a certain analyte.[26]

Following these results, we also decided to differently functionalize the two nitrogen donors of **L^1**. In particular, starting from **L^3** we prepared **L^4** and **L^5**, in which only one secondary nitrogen atom of **L^1** bears an anthracenylmethyl unit, whereas the other one features a pyridylmethyl and a 2,2-dimethyl-2-hydroxyethyl coordinating pendant arm (Figure 1). Potentiometric measurements in MeCN/H_2O (1:1 v/v) allowed the calculation of the protonation constants of **L^3**−**L^5** and the formation constants of their complexes with Cu^{II}, Zn^{II}, Cd^{II}, Hg^{II}, and Pb^{II}. Furthermore, the optical responses of **L^3**−**L^5** to the above-mentioned metal ions were measured as a function of pH in MeCN/H_2O (1:1 v/v) to study the effect, in terms of substrate-specific response, of the different binding domains determined by coordinating pendant arms.

Experimental Section

Instrument and Materials. All of the melting points are uncorrected. Microanalytical data were obtained using a Fison EA CHNS−O instrument operating at 1000 °C. ^1H and ^{13}C NMR spectra were recorded on a Varian VXR300 or a VXR400 spectrometer. Spectrophotometric measurements were carried out at 25 °C using a Varian Model Cary 5 UV−vis-NIR spectrophotometer or a PerkinElmer Lambda 25 spectrophotometer. Uncorrected emission and corrected excitation spectra were obtained with a Varian Cary Eclipse fluorescence spectrophotometer or a PerkinElmer LS-50 fluorescence spectrophotometer. To allow comparison among emission intensities, we performed corrections for instrumental response, inner filter effect, and phototube sensitivity.[27] A correction for differences in the refractive index was introduced where necessary. Luminescence quantum yields ($\lambda_{exc} = 367$ nm, uncertainty ± 15%) were determined using quinine sulfate in a 1 M H_2SO_4 aqueous solution ($\Phi = 0.546$) as a reference. For spectrophotometric measurements, MeCN (Uvasol, Merck) and Millipore grade water were used as solvents.

Fluorescent titrations of **L^3**−**L^5** at variable pH were performed by adding increasing volumes of 0.1 M NaOH in MeCN/H_2O (1:1 v/v) to an acidic solution of the ligand or its 1:1 metal−ion complex (MeCN/H_2O 1:1 v/v, 10 mL, $2.5 \times 10^{-5} - 2.5 \times 10^{-6}$ M) in the presence of aqueous 1 M 4-(2-hydroxyethyl)piperazine-1-ethanesulfonic acid (HEPES, 100 μL); the initial pH was adjusted by

---

(9) (a) Valeur, B.; Leray, I. *Coord. Chem. Rev.* **2000**, *205*, 3−40. (b) Métivier, R.; Leray, I.; Valeur, B. *Chem. Commun.* **2003**, 996−997.
(10) Freiria, A.; Bastida, R.; Valencia, L.; Macias, A.; Lodeiro, C. *Inorg. Chim. Acta* **2006**, *359*, 2383.
(11) Martínez-Máñez, R.; Sancenón, F. *Chem. Rev.* **2003**, *103*, 4419.
(12) Cho, I.; Chang, S.-K. *Chem. Lett.* **1981**, *4*, 515.
(13) Knockel, A.; Oeheler, J.; Rudolph, G.; Sinnwell, V. *Tetrahedron* **1977**, *33*, 119.
(14) Semnani, A.; Shamsipur, M. *J. Inclusion Phenom. and Mol. Recognit. Chem.* **1995**, *22*, 99.
(15) Arnold, K. A.; Hernandez, J. C.; Li, C.; Mallan, J. V.; Nakano, A.; Akio, S.; Schall, O. F.; Trafton, J. E.; Tsesarkaja, M.; White, B. D.; Gokel, G. W. *Supramol. Chem.* **1995**, *5*, 45.
(16) Buschmann, H.-J.; Schollmeyer, E.; Trueltzsch, R.; Beger, J. *Thermochim. Acta* **1993**, *213*, 11.
(17) Blair, T. L.; Desai, J.; Bachas, L. G. *Anal. Lett.* **1992**, *25*, 1823.
(18) Luboch, E.; Cyagan, A.; Bernat, J. *Inorg. Chim. Acta* **1983**, *68*, 201.
(19) Minta, A.; Tsien, R. Y. *J. Biol. Chem.* **1989**, *264*, 19449.
(20) Sammes, P. G.; Yahioglu, G.; Yearwood, G. D. *J. Chem. Soc., Chem. Commun.* **1992**, 1282.
(21) Xue, G.; Bradshaw, J. S.; Song, H.; Bronson, R. T.; Savage, P. B.; Krakowiak, K. E.; Izatt, R. M.; Prodi, L.; Montalti, M.; Zaccheroni, N. *Tetrahedron* **2001**, *57*, 87.
(22) Lloris, J. M.; Martínez-Máñez, R.; Padilla-Tosta, M.; Pardo, T.; Soto, J.; Beer, P. D.; Cadman, J.; Smith, D. K. *J. Chem. Soc., Dalton Trans.* **1999**, 2359.
(23) Al Shihadeh, Y.; Benito, A.; Lloris, J. M.; Martìnez-Màñez, R.; Pardo, T.; Soto, J.; Marcos Martìnez, M. D. *Polyhedron* **2000**, *19*, 1867.
(24) Al Shihadeh, Y.; Benito, A.; Lloris, J. M.; Martìnez-Màñez, R.; Pardo, T.; Soto, J.; Marcos, M. D. *J. Chem. Soc., Dalton Trans.* **2000**, 1199.
(25) Padilla-Tosta, M. E.; Lloris, J. M.; Martínez-Máñez, R.; Marcos, M. D.; Miranda, M. A.; Pardo, T.; Sancenón, F.; Soto, J. *Eur. J. Inorg. Chem.* **2001**, 1475.
(26) Sancenón, F.; Benito, A.; Hernández, F. J.; Lloris, J. M.; Martìnez-Màñez, R.; Pardo, T.; Soto, J. *Eur. J. Inorg. Chem.* **2002**, 866.
(27) Credi, A.; Prodi, L. *Spectrochim. Acta* **1998**, *54*, 159.

adding aqueous HCl (0.2 mL, 0.1 M). In each case, the effect of dilution on fluorescence emission was neglected. In the case of Hg^{II}, spectrofluorimetric titrations were performed in the absence of HEPES. L^1 was purchased from Aldrich Chemical Co., and other solvents and starting materials were purchased from commercial sources where available.

Caution! We crystallized the salt $[(H_2\mathbf{L^3})(H\mathbf{L^3})](ClO_4)_3$ from a MeCN solution of the crude perchlorate salt of $\mathbf{L^3}$ obtained by adding concentrated $HClO_4$ into a solution of $\mathbf{L^3}$ in EtOH. We worked with this product on a small scale without any explosive incidents. Despite this, the unpredictable behavior of perchlorate salts necessitates extreme care in handling.

Synthesis of 7-Anthracenylmethyl-1,4,10-trioxa-7,13-diazacyclopentadecane ($\mathbf{L^3}$). $\mathbf{L^3}$ was synthesized and isolated as described in the literature.[26] Here, we report for the first time its full characterization. Single crystals of $\mathbf{L^3}$ were grown by the diffusion of Et_2O vapor into a solution of the compound in EtOH. Anal. found (calcd for $C_{25}H_{32}N_2O_3$): C, 73.31 (73.50); H, 7.77 (7.90); N, 6.68 (6.86). ^1H NMR (400 MHz, $CDCl_3$) δ_H: 2.66 (s, 1H), 2.80−3.0 (m, 8H), 3.48−3.90 (m, 12 H), 4.71 (s, 2H), 7.50−7.80(m, 4H), 8.11 (d, $J = 8.4$, 2H), 8.52 (s, 1H), 8.67 (d, $J = 8.8$ Hz, 2H).^{13}C NMR (400 MHz, 298 K,$CDCl_3$) δ_C: 48.79, 49.02, 52.07, 53.44, 54.48, 69.40, 69.49, 69.80, 69.89, 70.21, 70.26, 124.70, 125.07, 125.50, 127.33, 128,78, 130.19, 131.26.

Synthesis of 7-Anthracenylmethyl-13-methylpyridyl-1,4,10-trioxa-7,13-diazacyclopentadecane ($\mathbf{L^4}$). A mixture of $\mathbf{L^3}$ (400 mg, 0.979 mmol) and (2-pyridylmethyl)chloride hydrochloride (200 mg, 1.24 mmol) in dry MeCN (20 mL) was refluxed under a N_2 atmosphere for 48 h in the presence of K_2CO_3 (690 mg, 4.96 mmol). The resulting orange solution was filtered, and the solvent was removed under reduced pressure. The yellow oil obtained was purified by chromatography on alumina using ethyl acetate as the eluant. $\mathbf{L^4}$ was obtained as a dark-orange viscous oil (350 mg, 0.7 mmol, 71.5% yield). Anal. found (calcd for $C_{31}H_{37}N_3O_3$): C, 74.41 (74.52); H, 7.41 (7.46); N, 8.60 (8.41). ^1H NMR (400 MHz, $CDCl_3$) δ_H: 2.05−2.30 (m, 2H), 2.70−2.90 (m, 3H), 2.95 (t, $J = 6$ Hz, 2H), 3.40−3.70 (m, 12 H), 3.79 (s, 2H), 4,56 (s, 2H), 7.0−7.12 (m, 2H), 7.38−7.60 (m, 6H), 7.95 (d, $J = 8$ Hz, 2H), 8.37 (s, 1H), 8.45−8.54 (m, 3H). ^{13}C NMR (300 MHz, $CDCl_3$) δ_C: 52.25, 53.76, 54.45, 54.52, 54.58, 62.08, 69.10, 69.34, 70.04, 70.40, 70.51, 70.54, 121.74, 123.02, 124.70, 125.16, 125.47, 127.36, 128.80, 130.30, 131.31, 136.31, 148.71, 159.96.

Synthesis of 7-Anthracenylmethyl-13-(2,2-dimethyl-2-hydroxyethyl)-1,4,10-trioxa-7,13-diazacyclopentadecane ($\mathbf{L^5}$). To a solution of $\mathbf{L^3}$ (190 mg, 0.465 mmol) in EtOH (10 mL) 1,2-epoxy-2-methylpropane (81.2 mg, 1.13 mmol, 0.1 mL) was added. The solution was stirred at room temperature for 20 days. The solvent was then removed under reduced pressure, and the residue (a yellow oil) was purified by chromatography on alumina using CH_2Cl_2/EtOH (100:2 v/v) as the eluant. The desired compound, $\mathbf{L^5}$, was isolated as a yellow oil (125 mg, 0.26 mmol, 56% yield). Anal. found (calcd for $C_{29}H_{40}N_2O_4$): C, 72.41 (72.46); H, 8.41 (8.39); N, 5.60 (5.83).^1H NMR (400 MHz, $CDCl_3$) δ_H: 1.17 (s, 6H), 2.42 (s, 2H), 2.70−3.0 (m, 8H), 3.3.40−3.70 (m, 12H), 4.2 (s, 1H), 4.57 (s, 2H), 7.38−7.52 (m, 4H), 7.96 (d, $J = 8$ Hz, 2H), 8.37 (s, 1H), 8.51 (d, $J = 8.8$ Hz, 2H). ^{13}C NMR (300 MHz, $CDCl_3$) δ_C: 27.43, 52.48, 53.88, 54.53, 57.98, 58.42, 67.36, 69.80, 69.96, 70.13, 70.28, 70.54, 70.67, 124.72, 125.14, 125.50, 127.37, 128.81, 130.33, 131.28, 131.31.

Synthesis of $[Cd\mathbf{L^3}(NO_3)_2]$. A solution of $Cd(NO_3)_2{\cdot}4H_2O$ (6.96 mg, 0.024 mmol) in MeCN (2 mL) was added to a solution of $\mathbf{L^3}$ (10 mg, 0.024 mmol) in MeCN (5 mL). The reaction mixture was stirred at room temperature for 3 h. The solvent was partially removed under reduced pressure, and crystals of the complex were obtained by diffusion of Et_2O vapor into the remaining solution (8.32 mg, 54% yield). Mp: 242 °C. Anal. found (calcd for $C_{25}H_{32}CdN_4O_9$): C, 46.65 (46.56); H, 4.97 (5.00); N, 8.61 (8.69).

Table 1. Crystallographic Data for $\mathbf{L^3}$, $[(H_2\mathbf{L^3})(H\mathbf{L^3})](ClO_4)_3$, and $[Cd\mathbf{L^3}(NO_3)_2]$

	$\mathbf{L}^3$	$[(H_2\mathbf{L^3})(H\mathbf{L^3})](ClO_4)_3$	$[Cd\mathbf{L^3}(NO_3)_2]$
formula	$C_{25}H_{32}N_2O_3$	$C_{50}H_{67}Cl_3N_4O_{18}$	$C_{25}H_{32}CdN_4O_9$
cryst syst	monoclinic	triclinic	monoclinic
space group	$P2_1/n$ (No. 14)	$P1$ (No. 1)[a]	$P2_1/c$ (No. 14)
mol wt	408.53	1118.43	644.95
a/Å	13.3963(13)	10.3932(10)	10.0206(5)
b/Å	12.3062(12)	11.8701(11)	7.8827(4)
c/Å	13.4509(13)	12.1822(12)	32.782(3)
α/deg		99.017(2)	
β/deg	93.300(2)	98.096(1)	92.210(5)
γ/deg		113.352(1)	
V/Å^3	2213.8(4)	1328.2(2)	2587.5(3)
Z	4	1	4
T/K	150(2)	150(2)	120(2)
D_c/g cm^{-3}	1.226	1.398	1.656
μ mm^{-1}	0.080	0.250	0.906
unique reflns, R_{int}	5031, 0.054	10272, 0.071	4031, 0.052
observed reflns [$I > 2\sigma(I)$]	3676	7793	2919
absorpion correction	none	none	*SADABS*[30]
T_{min}, T_{max}			0.8396, 0.9149
R1 [$I > 2\sigma(I)$]	0.0547	0.0565	0.0583
wR2 (all data)	0.1552	0.1321	0.2061

[a] Flack parameter is equal to 0.32(6).

Potentiometric Measurements. All of the pH measurements (pH $= -\log$ [H^+]) employed for the determination of ligand protonation and metal complex stability constants were carried out in a 0.10 M solution of NMe_4Cl in MeCN/H_2O (1:1 v/v) at 298.1 ± 0.1 K by means of conventional titration experiments under an inert atmosphere. The choice of the solvent mixture was dictated by the low solubility of the ligands in pure water. The combined Ingold 405 S7/120 electrode was calibrated as a hydrogen concentration probe by titrating known amounts of HCl with CO_2-free NMe_4OH solutions and determining the equivalent point by Gran's method,[28] which allows one to determine the standard potential $E°$ and the ionic product of water [$pK_w = 14.99(1)$ at 298.1 ± 0.1 K in 0.1 M NMe_4Cl]. At least three measurements (with about 100 data points for each one) were performed for each system in the pH range 2−11. In all of the experiments, the ligand concentration [$\mathbf{L}$] was about 1×10^{-3} M. In the complexation experiments, the metal ion concentration was [M^{II}] = 0.8[$\mathbf{L}$]. The computer program *HYPERQUAD*[29] was used to calculate the equilibrium constants from electromotive force data.

In the case of Hg^{II}, chloride strongly competes with ligands in metal complexation, and only minor percentages of the Hg^{II} complexes with $\mathbf{L^3}$−$\mathbf{L^5}$ were formed under our experimental conditions, precluding a reliable determination of their stability constants. Therefore, for this metal ion, the potentiometric measurements were performed in a different ionic medium (0.1 M NMe_4NO_3).

Crystallography. Crystal data and refinement details for the three structure determinations appear in Table 1. Only special features of the analyses are mentioned here. The single-crystal data for $[Cd\mathbf{L^3}(NO_3)_2]$ were collected via φ and ω scans on a Bruker-Nonius Kappa CCD diffractometer with a Bruker-Nonius FR591 rotating anode, equipped with an Oxford Cryosystem open-flow cryostat operating at 120 K. For $\mathbf{L^3}$ and $[(H_2\mathbf{L^3})(H\mathbf{L^3})](ClO_4)_3$, data

---

(28) Gran, G. *Analyst* **1952**, *77*, 661.

(29) Gans, P.; Sabatini, A.; Vacca, A. *Talanta* **1996**, *43*, 1739.

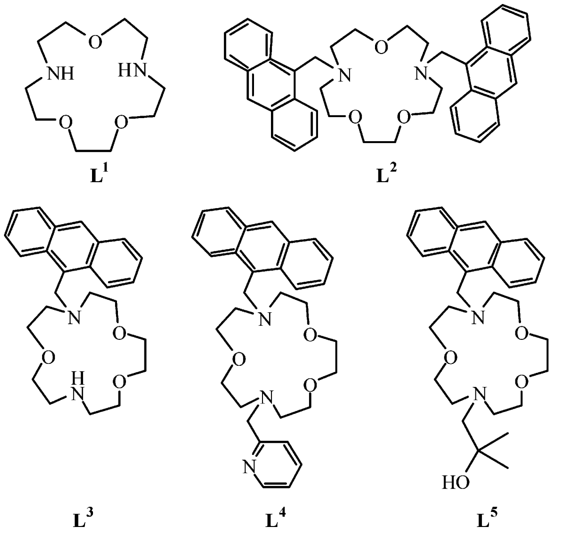

Figure 1. Fluorescent chemosensors based on $\mathbf{L^1}$ bearing anthracenylmethyl fragments.

were acquired via ω scans on a Bruker SMART APEX CCD diffractometer equipped with an Oxford Cryosystem open-flow cryostat operating at 150 K. Datasets were corrected for Lorentz-polarization effects and, where necessary, for absorption. The structures were solved by direct methods using *SHELXS-97*[31] and refined using *SHELXL-97*.[32] All non-hydrogen atoms were refined anisotropically. Hydrogen atoms were introduced at calculated positions and refined using a riding model, apart from those on secondary nitrogen atoms, which were located from difference maps and refined as part of rigid groups.

Results and Discussion

Synthesis and Coordination Properties of $\mathbf{L^3}$−$\mathbf{L^5}$. $\mathbf{L^3}$ was synthesized and isolated as described in the literature[26] by reacting $\mathbf{L^1}$ and 9-(chloromethyl)anthracene in CH_2Cl_2 in a 1:1 reaction molar ratio in the presence of triethylamine. However, this compound has only been used as a synthetic intermediate, and its full characterization has never been reported.[26] Crystals of $\mathbf{L^3}$ suitable for single-crystal X-ray diffraction analysis were obtained by slow diffusion of Et_2O vapor into a solution of the compound in ethyl alcohol. Part a of Figure 2 shows an ellipsoid plot for $\mathbf{L^3}$. The intramolecular distances are typical for this type of compound. The macrocyclic framework adopts a puckered conformation with 8 out of 15 torsion angles assuming an anti conformation. In particular, all of the C−O bonds assume anti arrangements [101.30(16)−176.07(15)°], whereas a gauche disposition is preferred at the C−C bonds [57.5(3)−81.64(16)°]. Of two torsion angles at each C−N bond, one assumes a gauche and the other assumes an anti arrangement. In this way, each of the five donor atoms of the macrocyclic framework assumes an endo orientation with respect to the ring cavity. The bifurcated intramolecular N(7)−H(7)···O(4)/O(10) hydrogen bonds (part a of Figure 2) also appear to favor this conformation.

Single crystals having the formulation $[H_3(\mathbf{L^3})_2](ClO_4)_3$ that are suitable for X-ray diffraction analysis were also obtained by slow diffusion of Et_2O vapor into a MeCN solution of the crude perchlorate salt of $\mathbf{L^3}$ that was obtained by adding concentrated $HClO_4$ into a solution of $\mathbf{L^3}$ in EtOH. An X-ray diffraction analysis revealed the compound to be the salt $[(H_2\mathbf{L^3})(H\mathbf{L^3})](ClO_4)_3$, in which two differently protonated $\mathbf{L^3}$ molecules are present in the asymmetric unit (part b of Figure 2). One is protonated on both nitrogen donor atoms of the macrocyclic framework, whereas the other is protonated only on the tertiary nitrogen donor atom. In both $(H_2\mathbf{L^3})^{2+}$ and $(H\mathbf{L^3})^{+}$ cations, the macrocyclic framework adopts a conformation very similar to that observed in the structure of neutral $\mathbf{L^3}$. In both cations, the hydrogen atom on both of the protonated tertiary nitrogen donors is involved in intramolecular bifurcated hydrogen bonds with the two proximal oxygen donors [O(4)/O(13) or O(4A)/O(13A)] from the respective macrocyclic framework (part b of Figure 2). The dication $(H_2\mathbf{L^3})^{2+}$ is linked to the monocation $(H\mathbf{L^3})^{+}$ by an intermolecular N−H···N hydrogen bond [H(7C)···N(7A) 1.904(12), N(7)···N(7A) 2.798(5) Å, N(7)−H(7C)−N(7A) 179(5)°]. Moreover, protons H(7B) and H(7A) are each involved in an intramolecular bifurcated hydrogen bond with the two proximal oxygen donors [O(4)/O(10) or O(4A)/O(10A), respectively] and an intermolecular hydrogen bond to a perchlorate anion to give four-centered hydrogen bonds (part b of Figure 2).

Both $\mathbf{L^4}$ and $\mathbf{L^5}$ were synthesized starting from $\mathbf{L^3}$. $\mathbf{L^4}$ was obtained by reacting $\mathbf{L^3}$ with (2-pyridylmethyl)chloride hydrochloride in MeCN in the presence of K_2CO_3. Following a procedure described in the literature,[33] the reaction of $\mathbf{L^3}$ with 1,2-epoxy-2-methylpropane in EtOH afforded $\mathbf{L^5}$ in good yield.

Protonation of $\mathbf{L^1}$ and $\mathbf{L^3}$−$\mathbf{L^5}$ and complex formation with Cu^{II}, Zn^{II}, Cd^{II}, and Pb^{II} were investigated by means of potentiometric measurements in $MeCN/H_2O$ (1:1 v:v, 298.1 K, 0.1 M NMe_4Cl) in the pH range 2−11. In the case of $\mathbf{L^3}$ and $\mathbf{L^5}$ with Cu^{II}, the low solubility of the complexes in the whole range of pH values explored precluded a speciation study by potentiometric measurements. The complex formation with Hg^{II} was studied in a 0.1 M NMe_4NO_3 ionic medium to avoid competitive coordination of Cl^- to the metal ion.

The protonation constants are supplied within the Supporting Information (Tables S1 and S2). For all of the ligands, two protonation steps are observed at slightly alkaline pH values. The values of the two corresponding basicity constants are in the range generally observed for the protonation of aliphatic amine compounds.[34] $\mathbf{L^1}$ and $\mathbf{L^3}$, however, display a somewhat higher first basicity constant than $\mathbf{L^4}$ and $\mathbf{L^5}$, due to the presence in $\mathbf{L^1}$ and $\mathbf{L^3}$ of secondary amine groups, which are more basic than tertiary ones. For the same reason, $\mathbf{L^1}$, which contains two secondary amines, shows the highest second protonation constant of the four

---

(30) *SADABS*, Area-Detector Absorption Correction Program; Bruker AXS, Inc.: Madison, WI, 2003.

(31) Sheldrick, G. M. *SHELXS 86−97*; *Acta Crystallogr. Sect. A* **1990**, *46*, 467.

(32) Sheldrick, G. M. *SHELXL 97−2*; University of Göttingen: Göttingen, Germany, 1998.

(33) Blake, A. J.; Danks, J. P.; Harrison, A.; Parsons, S.; Schooler, P.; Whittaker, G.; Schröder, M. *J. Chem. Soc., Dalton Trans.* **1998**, 2335.

(34) Bencini, A.; Bianchi, A.; Garcia-España, E.; Micheloni, M.; Ramirez, J. A. *Coord. Chem. Rev.* **1999**, *188*, 97.

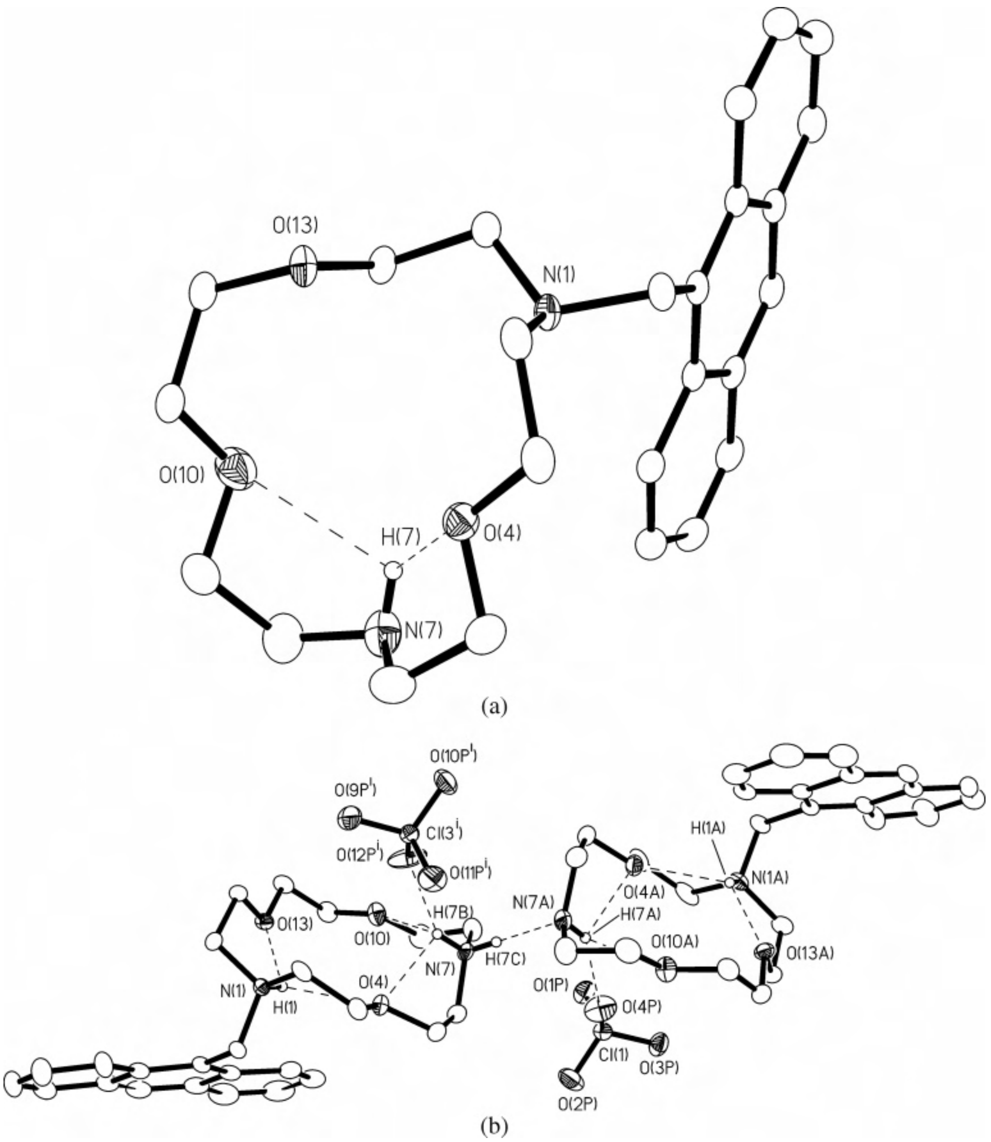

Figure 2. (a) *ORTEP* view of $\mathbf{L^3}$ with the numbering scheme adopted showing the bifurcated hydrogen bonds; all of the hydrogen atoms, except that on the secondary nitrogen donor, have been omitted for clarity. (b) *ORTEP* view of the cation $[(H_2\mathbf{L^3})(H\mathbf{L^3})]^{3+}$ interacting with two ClO_4^- anions in $[(H_2\mathbf{L^3})(H\mathbf{L^3})](ClO_4)_3$ with the numbering scheme adopted. Hydrogen atoms, except those on the nitrogen atoms, and the other two independent ClO_4^- anions in the asymmetric unit, have been omitted for clarity; $i = -1 + x, -1 + y, z$. Displacement ellipsoids are drawn at the 30% probability level. Hydrogen bond lengths and angles are reported as Supporting Information.

ligands. Finally, $\mathbf{L^4}$ displays a weak tendency to bind a third proton [log $K = 2.91(5)$ for the formation of the $(H_3\mathbf{L^4})^{3+}$ species], as expected considering that this protonation step would occur on the weakly basic pyridine nitrogen.

The complexes formed, and the corresponding stability constants are reported in Table 2. Precipitation of hydroxo complexes at alkaline pH values precluded the study of some systems in the alkaline pH region (Table 2). However, because the process of complex formation generally takes place at acidic pH values, the relevant stability constants of the 1:1 $[M\mathbf{L}]^{2+}$ species were determined in each case, with the only exceptions being the Cu^{II} complexes with $\mathbf{L^3}$ and $\mathbf{L^5}$.

The stability of the $[M\mathbf{L}]^{2+}$ complexes increases in the order $Zn^{II} < Cd^{II} < Pb^{II} < Cu^{II} < Hg^{II}$ the only exception being the Cd^{II} complex with $\mathbf{L^4}$, which is slightly more stable than the corresponding Pb^{II} one. As generally observed in the case of polyamine ligands, Hg^{II} and Cu^{II} form the most stable complexes, as a result of the remarkably high affinity of Hg^{II} for amine donors and the crystal field stabilization energy contribution to the stabilization of the Cu^{II} complexes. In contrast, the lower stability of the Zn^{II} complexes with respect to Cd^{II} and Pb^{II} ones is rather unusual for polyamine ligands, which often show a similar binding ability for these metal cations.[34] On the other hand, it has been reported that the cavities of 15-membered oxa−aza macrocycles are too large to optimally host small metal cations such as Zn^{II}.[35] The larger Cd^{II} and Pb^{II} ions achieve a better match with the dimensions of the macrocyclic cavity, and an overall stronger interaction with the N_2O_3-donor set, compared to Zn^{II}, leading to the observed higher stability of their complexes (see below for the crystal structure of the complex

---

(35) (a) Arnaud-Neu, F.; Spiess, B.; Schwing-Weill, M.-J. *Helv. Chim. Acta* **1977**, *60*, 2633. (b) Thom, V. J.; Shaikjee, M. S.; Hancock, R. D. *Inorg. Chem.* **1986**, *25*, 2992. (c) Hancock, R. D. *Pure Appl. Chem.* **1986**, *58*, 1445.

Table 2. Formation Constants (log *K*) of the Metal Complexes with $\mathbf{L}^1$ and $\mathbf{L}^3$–$\mathbf{L}^5$ in a MeCN/H_2O (1:1 v/v) Mixture ($I = 0.1$ M, 298.1 K)

equilibria	$Cu^{II\,a,b}$	$Zn^{II\,a}$	$Cd^{II\,a}$	$Pb^{II\,a}$	$Hg^{II\,c}$
$\mathbf{L}^1 + M^{2+} \rightleftharpoons [M\mathbf{L}^1]^{2+}$	8.61(5)	5.81(4)	6.52(4)	6.9(1)	13.2(1)
$[M\mathbf{L}^1]^{2+} + OH^- \rightleftharpoons [M\mathbf{L}^1(OH)]^+$	5.3(1)	6.3(1)	6.1(1)	6.8(1)	6.0(1)
$[M\mathbf{L}^1(OH)]^+ + OH^- \rightleftharpoons [M\mathbf{L}^1(OH)_2]$	5.1(1)	5.5(1)	5.5(1)	5.9(1)	5.8(1)
$\mathbf{L}^3 + M^{2+} \rightleftharpoons [M\mathbf{L}^3]^{2+}$		3.8(1)	4.6(1)	6.31(3)	11.1(1)
$[M\mathbf{L}^3]^{2+} + OH^- \rightleftharpoons [M\mathbf{L}^3(OH)]^+$		7.2(1)[d]	6.0(1)[d]	6.48(8)	6.5(1)
$[M\mathbf{L}^3(OH)]^{2+} + OH^- \rightleftharpoons [M\mathbf{L}^3(OH)_2]$				4.9(1)	4.9(1)
$\mathbf{L}^4 + M^{2+} \rightleftharpoons [M\mathbf{L}^4]^{2+}$	7.89(4)	4.4(1)	7.7(1)	7.3(1)[d]	12.2(1)[d]
$[M\mathbf{L}^4]^{2+} + H^+ \rightleftharpoons [M(H\mathbf{L}^4)]^{3+}$	6.38(3)[d]				
$[M\mathbf{L}^4]^{2+} + OH^- \rightleftharpoons [M\mathbf{L}^4(OH)]^+$		6.1(1)	7.2(1)[d]		
$[M\mathbf{L}^4(OH)]^+ + OH^- \rightleftharpoons [M\mathbf{L}^4(OH)_2]$		6.6(1)			
$\mathbf{L}^5 + M^{2+} \rightleftharpoons [M\mathbf{L}^5]^{2+}$		4.1(1)	5.0(1)[d]	6.06(4)	10.8(1)
$[M\mathbf{L}^5]^{2+} + OH^- \rightleftharpoons [M\mathbf{L}^5(OH)]^+$		6.9(1)[d]		7.5(1)[d]	7.8(1)
$[M\mathbf{L}^5(OH)]^+ + OH^- \rightleftharpoons [M\mathbf{L}^5(OH)_2]$					6.2(1)

[a] Measurements carried out in 0.1 M NMe_4Cl. [b] Low solubility of the Cu^{II} complexes with $\mathbf{L}^3$ and $\mathbf{L}^5$ does not allow the potentiometric study of these systems. [c] Measurements carried out in 0.1 M NMe_4NO_3. [d] Precipitation at slightly alkaline pH values of hydroxo complexes does not allow the study of the system above pH 8.

$[Cd\mathbf{L}^3(NO_3)_2]$). Comparing the binding ability of the four ligands, the data in Table 2 show that the stabilities of the 1:1 complexes generally increase in the order $\mathbf{L}^3 \cong \mathbf{L}^5 < \mathbf{L}^4 < \mathbf{L}^1$, the only exceptions being the Cd(II) and Pb(II) complexes with $\mathbf{L}^4$, which are somewhat more stable than those with $\mathbf{L}^1$. The superior binding abilities of $\mathbf{L}^1$ can be ascribed to the presence within the macrocyclic framework of two secondary nitrogen donors, which are better σ donors than tertiary ones. In fact, it is known that nitrogen alkylation reduces the σ-donating properties of amine groups; the absence of $M-N(R)_2-H\cdots OH_2$ hydrogen bonds to the solvent makes tertiary amino groups even weaker σ donors.[36] Furthermore, steric hindrance due to the functionalization of the amine donors with large alkyl or alkyl–aryl units can cause elongation of the M–N bonds and distortions of the coordination sphere of the metal, thus reducing the overall metal–ligand interaction.

In this respect, $\mathbf{L}^3$ would be expected to give more stable complexes than $\mathbf{L}^4$ and $\mathbf{L}^5$, as a result of the presence in $\mathbf{L}^3$ of a secondary nitrogen donor. The observed trend ($\mathbf{L}^3 \cong \mathbf{L}^5 < \mathbf{L}^4$) can be related to the potential coordinative ability of the side arms of $\mathbf{L}^4$ and $\mathbf{L}^5$, which contain respectively a pyridine nitrogen and an alcoholic oxygen donor. In particular, the higher stability displayed by the complexes with $\mathbf{L}^4$ can be attributed to the involvement of the pyridine nitrogen in metal coordination, as already observed in other macrocyclic compounds containing appended pyridine rings.[37]

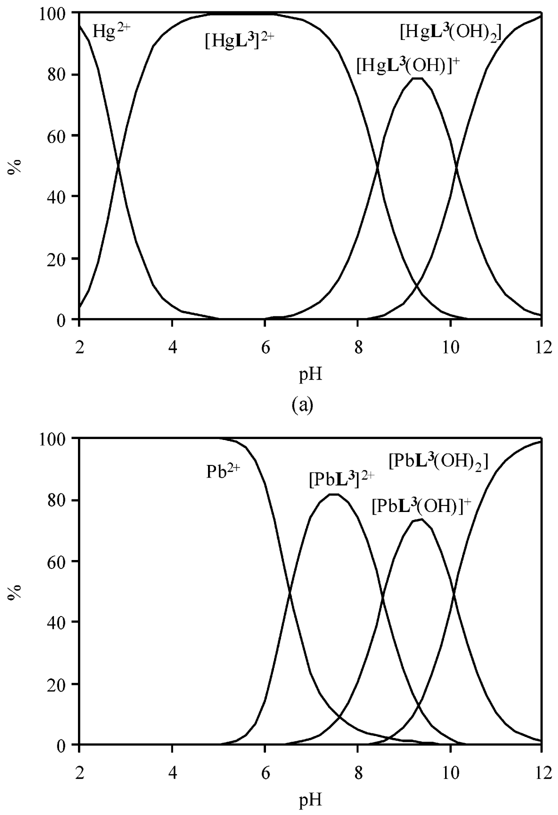

(a)

(b)

Figure 3. Distribution diagrams for the systems $Hg^{II}/\mathbf{L}^3$ (a) and $Pb^{II}/\mathbf{L}^3$ (b) in MeCN/H_2O (1:1 v/v) [$I = 0.1$ M (Me_4NCl for Pb^{II}, Me_4NNO_3 for Hg^{II}), 298.1 K, $[M^{II}] = 0.8[\mathbf{L}]$, $[\mathbf{L}^3] = 1 \times 10^{-3}$ M].

Unfortunately, despite many attempts, we were not able to obtain the crystal structure of any metal complexes with $\mathbf{L}^4$. The oxygen donor of the alcoholic side arm in $\mathbf{L}^5$ has weaker binding ability toward transition and post-transition metals than a pyridine nitrogen and, therefore, the 1:1 complexes with $\mathbf{L}^5$ are less stable than those with $\mathbf{L}^4$. However, the observed similar stability of the 1:1 complexes with $\mathbf{L}^3$ and $\mathbf{L}^5$ suggests that an interaction of the pendant alcoholic group with the metals, even if weak, does occur and compensates for the replacement of the secondary amine group in $\mathbf{L}^3$ with the poorer σ-donor tertiary nitrogen in $\mathbf{L}^5$.

In general, for all of the metal ions considered, the formation of 1:1 complexes $[M\mathbf{L}]^{2+}$ takes place at slightly acidic or neutral pH values and is followed by a facile deprotonation of coordinated water molecules to afford mono- and/or dihydroxo complexes as shown in Figure 3 for the systems $Pb^{II}/\mathbf{L}^3$ and $Hg^{II}/\mathbf{L}^3$. The constants for the successive addition of hydroxide anions to the $[M\mathbf{L}]^{2+}$ complexes ($\mathbf{L} = \mathbf{L}^1$, $\mathbf{L}^3$–$\mathbf{L}^5$) are remarkably high, ranging from 4.9 to 7.8 log units. As a consequence, large amounts of hydroxo complexes are generally formed in the alkaline pH region. This behavior is generally attributed to a metal coordination environment that is not saturated by the ligand donors, probably due to the presence of ether oxygen atoms, which are at most only weakly bound to the metals in solution. Only for the $Cu^{II}/\mathbf{L}^4$ system did we observe for the 1:1 complex a marked tendency to bind a proton to afford the monoprotonated $[Cu(H\mathbf{L}^4)]^{3+}$ species (Table 2).

---

(36) (a) Meyerstein, D. *Coord. Chem. Rev.* **1999**, *185–186*, 141. (b) Clark, T.; Hennemann, M.; van Eldik, R.; Meyerstein, D. *Inorg. Chem.* **2002**, *41*, 2927. (c) Golub, G.; Cohen, H.; Paoletti, P.; Bencini, A.; Messori, L.; Bertini, I.; Meyerstein, D. *J. Am. Chem. Soc.* **1995**, *117*, 8353. (d) Golub, G.; Cohen, H.; Meyerstein, D. *J. Chem. Soc., Chem. Commun.* **1992**, 398.

(37) (a) Kimura, E.; Kotache, Y.; Koike, T.; Shionoya, M.; Shiro, M. *Inorg. Chem.* **1990**, *29*, 4991. (b) Kimura, E.; Koike, T.; Machida, R.; Nagai, R.; Kodama, M. *Inorg. Chem.* **1984**, *23*, 4181. (c) Vuckovic, G.; Asato, E.; Matsumoto, N.; Kida, S. *Inorg. Chim. Acta* **1990**, *171*, 45. (d) Asato, E.; Toflund, H.; Kida, S.; Mikuriya, M.; Murray, K. S. *Inorg. Chim. Acta* **1989**, *165*, 207. (e) Damu, K. V.; Shaikjee, M. S.; Michael, J. P.; Howard, A. S.; Hancock, R. D. *Inorg. Chem.* **1986**, *25*, 3879. (f) Bazzicalupi, C.; Bencini, A.; Bianchi, A.; Fedi, V.; Fusi, V.; Giorgi, C.; Paoletti, P.; Tei, L.; Valtancoli, B. *J. Chem. Soc., Dalton Trans.* **1999**, 1101.

Table 3. Selected Bond Distances (Angstroms) and Angles (Degrees) for $[\mathrm{Cd}\mathbf{L}^3(\mathrm{NO}_3)_2]^{a,b}$

Cd(1)−N(1)	2.591(4)	Cd(1)−O(13)	2.484(3)
Cd(1)−N(7)	2.337(5)	Cd(1)−X	2.354(3) [2.512(4)]
Cd(1)−O(4)	2.411(3)	Cd(1)−O(4S)	2.336(4)
Cd(1)−O(10)	2.602(3)		
N(1)−Cd(1)−N(7)	140.87(13)	O(4)−Cd(1)−O(10)	122.33(11)
N(1)−Cd(1)−O(4)	69.47(11)	O(4)−Cd(1)−O(13)	95.24(11)
N(1)−Cd(1)−O(10)	132.31(11)	O(4)−Cd(1)−X	153.74(11)[143.55(13)]
N(1)−Cd(1)−O(13)	68.30(11)	O(4)−Cd(1)−O(4S)	84.77(12)
N(1)−Cd(1)−X	85.73(12) [133.18(13)]	O(10)−Cd(1)−O(13)	74.79(11)
N(1)−Cd(1)−O(4S)	84.02(14)	O(10)−Cd(1)−X	80.64(10) [67.73(12)]
N(7)−Cd(1)−O(4)	71.44(13)	O(10)−Cd(1)−O(4S)	138.69(14)
N(7)−Cd(1)−O(10)	70.12(12)	O(13)−Cd(1)−X	82.92(12) [118.67(11)]
N(7)−Cd(1)−O(13)	114.20(13)	O(13)−Cd(1)−O(4S)	150.17(14)
N(7)−Cd(1)−X	133.11(14) [82.00(15)]	O(4S)−Cd(1)−X	84.18(12) [72.47(13)]
N(7)−Cd(1)−O(4S)	94.15(15)	O(1S)−Cd(1)−O(2S)	52.74(13)

[a] X = N(1S)O$_3$. [b] Where two values are reported, the first refers to bond distances and angles involving O(1S), and the second refers to bond distances and angles involving O(2S).

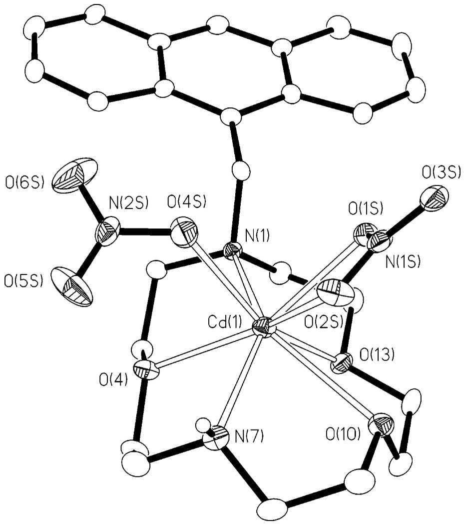

Figure 4. *ORTEP* view of the complex $[\mathrm{Cd}\mathbf{L}^3(\mathrm{NO}_3)_2]$. All of the hydrogen atoms, except that on the secondary nitrogen donor, have been omitted for clarity. Displacement ellipsoids are drawn at the 30% probability level.

Despite numerous attempts to isolate crystals of the 1:1 complexes of $\mathbf{L}^3-\mathbf{L}^5$ with the metal ions under investigation, only for $[\mathrm{Cd}\mathbf{L}^3(\mathrm{NO}_3)_2]$ were we able to grow crystals of diffraction quality. In this complex, the metal center is eight-coordinated, and its coordination sphere consists of the N_2O_3-donor set of the macrocyclic framework of $\mathbf{L}^3$, and a monodentate and an asymmetrically bidentate nitrato ligand (Figure 4, Table 3). The two Cd−N bond distances are significantly different, with that involving the tertiary nitrogen [2.591(4) Å], bearing the anthracenylmethyl pendant arm, being longer than that with the secondary amino group [2.337(5) Å]. On the other hand, the Cd−O$_{\mathrm{nitrato}}$ distances are on average shorter than the bond lengths between the metal center and the oxygen atoms of the macrocyclic moiety (Table 3). Although it strongly interacts with all of the donor atoms from the macrocyclic framework, the metal ion is displaced out of the ring cavity [0.93 Å out of the mean plane defined by the atoms N(1), N(7), O(4), O(10), O(13)] by the interaction with the nitrato ligands. The conformation of the macrocyclic portion is not significantly modified by the coordination of the metal ion with respect to free $\mathbf{L}^3$. $[\mathrm{Cd}\mathbf{L}^3(\mathrm{NO}_3)_2]$ molecules are hydrogen bonded into dimers [N(7)−H(7)···O(2S^i) 2.12, N(7)···O(2S^i) 2.972(6) Å, N(7)−H(7)−O(2S^i) 156°; $i = 1 - x, 2 - y, -z$].

Cation-Sensing Investigations. The following study was carried out to ascertain the potential usefulness of $\mathbf{L}^3-\mathbf{L}^5$ as selective and specific fluorescent chemosensors and to analyze, in this respect, the influence of the coordinating pendant arm in $\mathbf{L}^4$ and $\mathbf{L}^5$. The fluorescence behavior of $\mathbf{L}^3-\mathbf{L}^5$ in the absence and in the presence of Cu$^{\mathrm{II}}$, Zn$^{\mathrm{II}}$, Cd$^{\mathrm{II}}$, Hg$^{\mathrm{II}}$, or Pb$^{\mathrm{II}}$ (1:1 molar ratio) was studied as a function of the pH in the same solvent mixture (MeCN/H$_2$O 1:1 v/v), as was used for the potentiometric measurements.

Spectrofluorimetric titrations were performed by adding increasing volumes of 0.1 M NaOH in MeCN/H$_2$O (1:1 v/v) to an acidic solution of the free ligand or its 1:1 metal complex in MeCN/H$_2$O (1:1 v/v), in the presence of HEPES [4-(2-hydroxyethyl)piperazine-1-ethanesulfonic acid]. In the case of Hg$^{\mathrm{II}}$, spectrofluorimetric titrations were performed in absence of HEPES because of the ability of this compound to coordinate Hg$^{\mathrm{II}}$ ($\log K = 7.45$ for the formation of the complex [Hg(HEPES)]$^+$ under our experimental conditions). Each of the three ligands shows the typical structured absorption and emission spectra of anthracenyl groups, with a maximum in the absorption band at 367 nm and a maximum in the emission fluorescent band at ca. 420 nm (photophysical data including quantum yield values are supplied within the Supporting Information, Table S3).

The intensity of the fluorescence emission of $\mathbf{L}^3-\mathbf{L}^5$ is pH-dependent and decreases at basic pH values. This behavior for anthracenylmethyl functionalized polyamines is well-known, and it is determined by a PET process between the tertiary nitrogen donor atom of the macrocyclic framework to which the fluorescent unit is linked and the photoexcited state of anthracene moiety; the reducing properties of the tertiary nitrogen atom diminish with protonation at low pH values, thus suppressing this quenching mechanism.[26,38]

Figure 5 shows the pH dependence of the emission intensity at ca. 420 nm of $\mathbf{L}^3-\mathbf{L}^5$, superimposed on the distribution diagram of the protonated species of each ligand.

---

(38) (a) de Silva, P.; Gunnlaugsson, T.; Rice, T. E. *Analyst* **1996**, *121*, 1759. (b) Fabbrizzi, L.; Licchelli, M.; Pallavicini, P.; Sacchi, D.; Taglietti, A. *Analyst* **1996**, *121*, 1763.

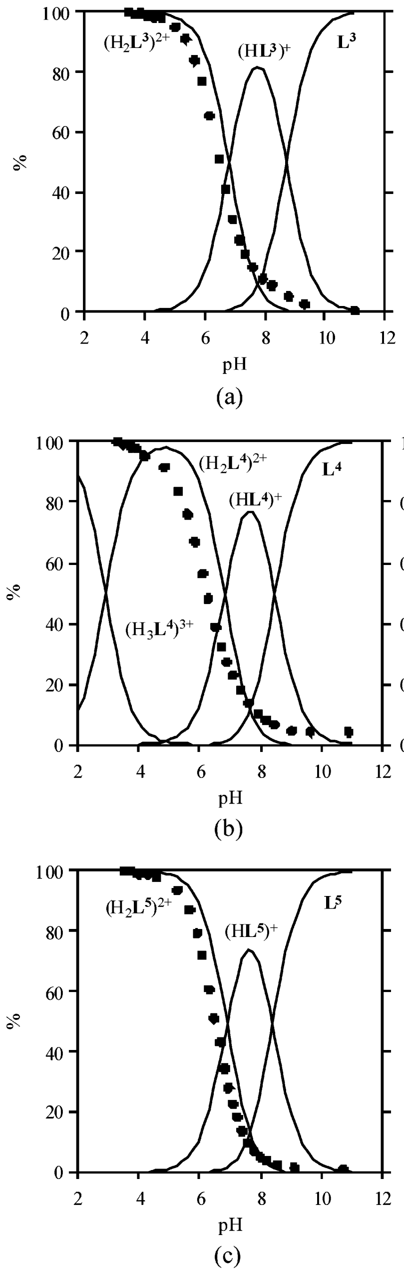

(a)

(b)

(c)

Figure 5. Relative fluorescence intensity versus pH for $\mathbf{L}^3$ (a), $\mathbf{L}^4$ (b), and $\mathbf{L}^5$ (c) (●, right *y* axis) ([**L**] = 2.5×10^{-5} M, MeCN/H_2O 1:1 v/v, 298.1 K, in the presence of HEPES; λ_{exc} 367 nm, λ_{em} 422 nm), superimposed to the distribution diagrams of the protonated species of the ligands (full line).

For each of the three ligands the diprotonated species is the emitting species, and the fluorescent emission intensity gradually decreases upon passing to the neutral forms via the monoprotonated species (Figure 5). In the case of $\mathbf{L}^4$, the protonation of the methylpyridyl pendant arm to afford $(H_3\mathbf{L}^4)^{3+}$ does not seem to affect the fluorescence emission intensity of the ligand.

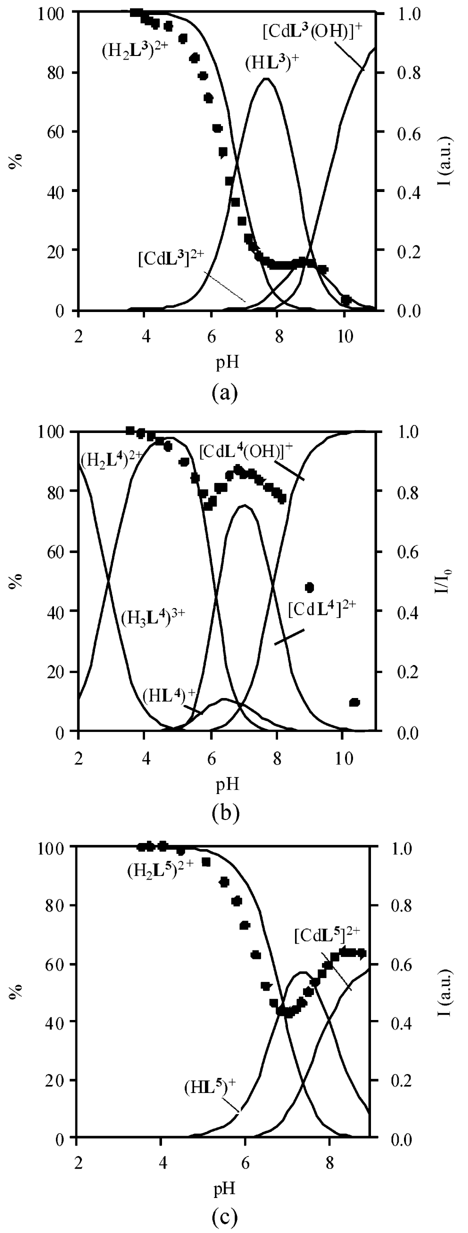

(a)

(b)

(c)

Figure 6. Relative fluorescence intensity versus pH for the systems Cd^{II}/$\mathbf{L}^3$ (a), Cd^{II}/$\mathbf{L}^4$ (b), and Cd^{II}/$\mathbf{L}^5$ (c) (●, right *y* axis) ([$\mathbf{L}^3$] = [$\mathbf{L}^4$] = [$\mathbf{L}^5$] = [Cd^{II}] = 2.5×10^{-5} M, MeCN/H_2O 1:1 v/v, 298.1 K, in the presence of HEPES; λ_{exc} 367 nm, λ_{em} 422 nm), superimposed to the distribution diagrams of the complex species of the ligands (full line).

Figures 6 and 7 show respectively the relative emission intensity in the presence of Cd^{II} for $\mathbf{L}^3$−$\mathbf{L}^5$ and in the presence of Zn^{II} for $\mathbf{L}^4$, as a function of the pH (1:1 metal-to-ligand molar ratio). In fact, Cd^{II} is the only metal ion to produce a clear enhancement of the fluorescent emission (CHEF) of $\mathbf{L}^3$ and $\mathbf{L}^5$ in the pH range 8−10 (parts a and c of Figure 6). For $\mathbf{L}^4$, the presence of either Zn^{II} or Cd^{II} causes a significant enhancement of the fluorescence band in the pH range 6−9 (part b of Figure 6 and Figure 7). The Cu^{II}, Pb^{II}, and Hg^{II} complexes with each of the three ligands, in contrast, are not emissive. As shown in Figure 8 for the systems Pb^{II}/$\mathbf{L}^3$, Cu^{II}/$\mathbf{L}^4$, and Hg^{II}/$\mathbf{L}^5$, the formation of these complexes is accompanied by a quenching of the fluorescence emission intensity, which actually follows the distribution curve of the diprotonated ligand (the same behavior is observed for the other M^{II}/**L** systems, including Zn^{II}/$\mathbf{L}^3$ and Zn^{II}/$\mathbf{L}^5$, and the corresponding distribution diagrams superimposed to the fluorimetric data are available from the authors, on request).

The effects of metal−ion complexation on the absorption properties of $\mathbf{L}^3$−$\mathbf{L}^5$ at pH values corresponding to the maximum formation of the 1:1 $[M\mathbf{L}]^{2+}$ species in the

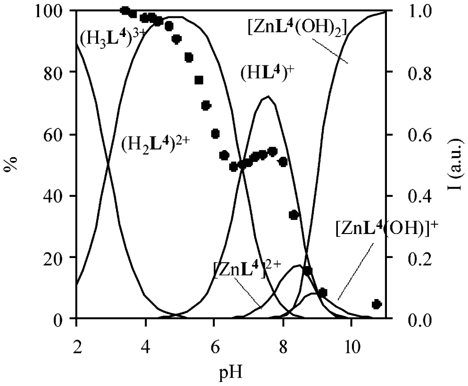

Figure 7. Relative fluorescence intensity versus pH for the systems Zn^{II}/L^4 (●, right y axis) ($[L^4] = [Zn^{II}] = 2.5 \times 10^{-5}$ M, $MeCN/H_2O$ 1:1 v/v, 298.1 K, in the presence of HEPES; λ_{exc} 367 nm, λ_{em} 422 nm), superimposed to the distribution diagram of the complex species of the ligand (full line).

distribution diagram from potentiometric studies were, in general, not dramatic. Small decreases in the extinction coefficients were observed in the case of Zn^{II}, Cd^{II}, and Pb^{II} (Figure S1 in the Supporting Information, for the case of Pb^{II}). In the case of Cu^{II} and Hg^{II}, the observed absorption decreases were generally more marked, and, with $\mathbf{L^4}$, they were also accompanied by a significant red-shift (Figures S2 and S3 in the Supporting Information).

The fluorescence enhancement effect in the pH range 8−10 produced specifically by the presence of Cd^{II} in the case of $\mathbf{L^5}$ is larger than that observed in the case of $\mathbf{L^3}$. At the same time, Cd^{II} also seems to cause, in the pH range 6−9, a fluorescent enhancement effect larger than that caused by Zn^{II} in the case of $\mathbf{L^4}$, and, furthermore, its effect on the fluorescence intensity of $\mathbf{L^4}$ is much more pronounced than that caused on the fluorescence intensities of $\mathbf{L^3}$ and $\mathbf{L^5}$.[39] Figures 6 and 7 suggest that the specific CHEF effect determined by Cd^{II} for $\mathbf{L^3}$ and $\mathbf{L^5}$, and by both Cd^{II} and Zn^{II} for $\mathbf{L^4}$, is associated with the presence in solution of 1:1 $[M\mathbf{L}]^{2+}$ complexes, whereas mono- and dihydroxylate species do not increase the fluorescence emission intensity of the free ligands. The different magnitude of the fluorescent enhancement effects observed for $\mathbf{L^3}$−$\mathbf{L^5}$ in the presence of Cd^{II} or Zn^{II} is also determined by the diverse percentage of 1:1 $[M\mathbf{L}]^{2+}$ complex species ($M = Cd^{II}, Zn^{II}$) present in solution.

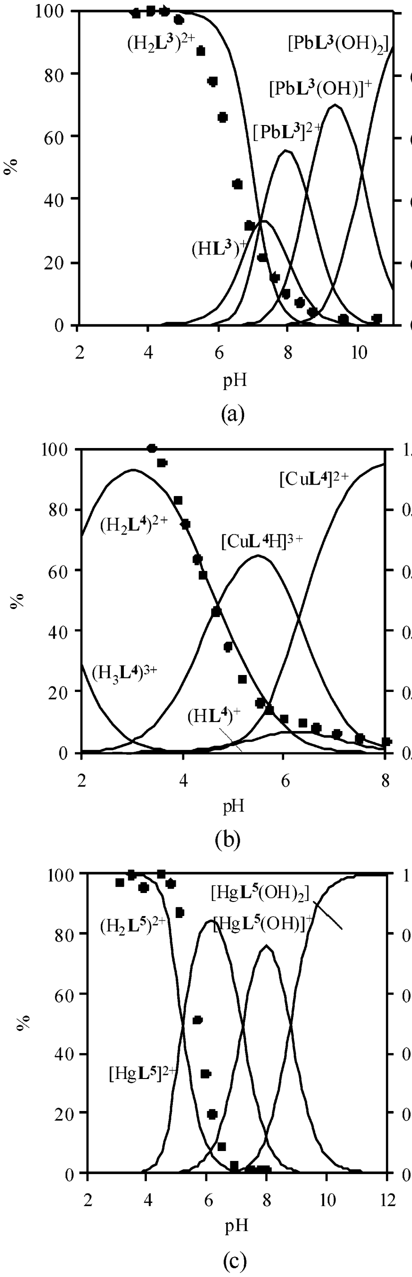

(a)

(b)

(c)

Figure 8. Relative fluorescence intensity versus pH for the systems Pb^{II}/L^3 (a), Cu^{II}/L^4 (b), and Hg^{II}/L^5 (c) (●, right y axis) ($[L^3] = [L^4] = [Pb^{II}] = [Cu^{II}] = 2.5 \times 10^{-5}$ M, $MeCN/H_2O$ 1:1 v/v, 298.1 K, in the presence of HEPES; $[L^5] = [Hg^{II}] = 2.5 \times 10^{-6}$ M, in the absence of HEPES; λ_{exc} 367 nm, λ_{em} 422 nm), superimposed to the distribution diagrams of the complex species of the ligands (full line).

It is also interesting that only Cd^{II} and Zn^{II}, which are the metal ions showing lower formation constants with $\mathbf{L^3}$−$\mathbf{L^5}$, are capable of giving emissive complexes. The fact that Cu^{II}, Hg^{II}, and Pb^{II} complexes are not emissive might be due to the strength of the interaction between each nitrogen atom in the macrocyclic framework and the metal cation, independently of the value of the formation constant for the 1:1 complex. In principle, a weaker coordination with at least one nitrogen atom in the ring will not hinder the PET process from the lone pair of the nitrogen atom to the excited fluorophore.[24,26] The binding affinity, however, is not the only factor to take into consideration. In fact, the observed optical response of anthracene-based fluorescence chemosensors is generally the result of a delicate balance between two main effects: (1) an increase in the luminescence because of the switching off of the eT process between the nitrogen atom and the adjacent excited anthracene unit upon metal coordination (this effect is expected for d^{10} metal ions such as Zn^{II}, Cd^{II}, Hg^{II}, and Pb^{II}) and (2) a quenching of the fluorescence due to either eT and ET processes involving the metal ions that introduce low-energy metal-centered or charge-separated excited states into the system (Cu^{II}) or to a heavy-atom effect (Hg^{II} and Pb^{II}). This second effect could also explain the lack of fluorescence emission of the Cu^{II}, Hg^{II}, and Pb^{II} complexes with $\mathbf{L^3}$−$\mathbf{L^5}$.

---

(39) The lack of perfect superimposition of the spectrofluorimetric curves to the distribution diagrams might be because the ionic media in the two types of experiments were different (Experimental Section).

Significantly, it has also been reported that only Hg^{II} is specifically able to produce an enhancement of the fluorescence emission intensity of **L^2**, which features the same macrocyclic receptor unit as **L^3**−**L^5** and bears two anthracenylmethyl pendant arms (Figure 1), in the pH range 5−9, in 1,4-dioxane/H_2O (70:30 v/v, 298 K, 0.1 M KNO_3).[24] In this solvent mixture, the metal ions Ni^{II}, Cu^{II}, Zn^{II}, Cd^{II}, and Pb^{II} are unable to modify the relative intensity versus pH profile of the free of **L^2**.[24]

Conclusions

Two new fluorescent chemosensors, **L^4** and **L^5**, based on the N_2O_3-donating macrocycle, **L^1**, and both characterized by an anthracenyl subunit, were synthesized. With respect to **L^3**, they are characterized by different functionalized pendant arms on the remaining secondary nitrogen donor.

The coordination chemistry of **L^3**−**L^5** toward Cu^{II}, Zn^{II}, Cd^{II}, Hg^{II}, and Pb^{II} in MeCN/H_2O (1:1 v/v) was studied potentiometrically, and their cation-sensing ability toward the same set of metal ions was investigated as a function of pH by spectrofluorimetric titrations, in the same solvent mixture.

The results clearly indicate the crucial importance of the topology and nature of the binding domain in the recognition process for anthracenyl derivatives of aza−oxa macrocyclic ligands, in particular, and conjugated fluorescent chemosensors that bear uncoordinating signaling units, in general. In particular, the role of the coordinating pendant arms seems to be fundamental in determining a specific response of the class of fluorescent chemosensors considered, on the basis of **L^1**, toward heavy metal ions.

In fact, in our experimental conditions, a specific CHEF effect is observed only for **L^3** and **L^5** with Cd^{II}, and for **L^4** with both Cd^{II} and Zn^{II} at basic pH values. In contrast, from the literature it was known that **L^2**, featuring two anthracenyl subunits anchored to **L^1**, responds only to Hg^{II} in a medium [1,4-dioxane/H_2O (70:30 v/v)], however, which is different from that we have used.[24]

In this context, it is important to recall that so far only a few examples of fluorescent chemosensors for Cd^{II} have been reported; the main challenge in this field is to find fluorescent systems that can discriminate between Cd^{II} and Zn^{II}.[40] Generally these two metal ions, which belong to the same group of the periodic table, have very similar chemical properties and cause similar spectral changes after interactions with fluorescent chemosensors. The approach to solving this discrimination problem by tuning the binding domain of macrocyclic receptor units appears, therefore, to still be worthwhile.

Acknowledgment. We thank the Ministero Italiano dell'Università e della Ricerca Scientifica e Tecnologica for funding for the Varian Cary Eclipse Fluorescence spectrophotometer, and EPSRC (U.K.) for support.

Supporting Information Available: Selected hydrogen bonds distances (angstroms) and angles (degrees) in **L^3** and [(H_2**L^3**)(H**L^3**)]-$(ClO_4)_3$; protonation constant (Table S1) of **L^1**, **L^3**−**L^5** in a MeCN/H_2O (1:1 v/v) mixture (0.1 M NMe_4Cl, 298.1 K); protonation constant (Table S2) of **L^1** and **L^3**−**L^5** in a MeCN/H_2O (1:1 v/v) mixture (0.1 M NMe_4NO_3, 298.1 K); photophysical parameters (Table S3) for **L^3** −**L^5** in MeCN/H_2O (1:1 v/v); UV absorption spectra of **L^3**, **L^4**, and **L^5** at pH 7.8 in the presence of increasing amounts of Pb^{II} (Figure S1); UV−vis absorption spectra of **L^4** at pH 7.5 in the presence of increasing amounts of Cu^{II} (Figure S2); UV−vis absorption spectra of **L^3**, **L^4**, and **L^5** at pH 7 in the presence of increasing amounts of Hg^{II} (Figure S3), in MeCN/H_2O 1:1 v/v; crystallographic data in CIF format. This material is available free of charge via the Internet at http://pubs.acs.org.

IC700657J

---

(40) (a) Peng, X.; Du, J.; Fan, J.; Wang, J.; Wu, Y.; Zhao, J.; Sun, S.; Xu, T. J. *Am. Chem. Soc.* **2007**, *129*, 1500; Lu, C.; Xu, Z.; Cui, J.; Zhang, R.; Qian, X. *J. Org. Chem.* **2007**, *72*, 3554.